Structural Control in Germania Hybrid Organic−Inorganic Materials

Bruno Alonso and Dominique Massiot

CRMHT, CNRS UPR 4212, 1D av. de la Recherche Scientifique, 45071 Orléans Cedex 2, France

Florence Babonneau

Chimie de la Matière Condensée, Université Paris 6 T54 E5, 4 place Jussieu, 75252 Paris Cedex 05 France

Giovanna Brusatin and Gioia Della Giustina

Dipartimento di Ingegneria Meccanica, Settore Materiali, Università di Padova, via Marzolo 9, 35131, Padova, Italy

Tongjit Kidchob and Plinio Innocenzi*

Dipartimento di Architettura e Pianificazione, Laboratorio di Scienza dei Materiali e Nanotecnologie, Nanoworld Institute, Università di Sassari, Palazzo Pou Salid, Piazza Duomo 6, 07041 Alghero, Sassari, Italy

Received December 20, 2004. Revised Manuscript Received March 3, 2005

The preparation of highly homogeneous hybrid organic−inorganic materials with enhanced functional properties requires a deep understanding of the synthesis process and a high control of the material structure. To achieve this goal it is necessary to apply advanced characterization techniques that can elucidate all the different features of a structure that is complicated by the presence of interconnected organic and inorganic species that cooperate in the building of a complex hybrid network. We have used as a case study a sol−gel synthesized germania−silica hybrid organic−inorganic material with a content of germania up to 30% in molar concentration with respect to silica. The material has been prepared using 3-glycidoxypropyltrimethoxysilane (GPTMS) as the organically modified alkoxide. Solid-state nuclear magnetic resonance (NMR) spectroscopy, coupled with infrared and Raman spectroscopies, has been used to investigate the structure of the material. In the samples prepared without germania or with a germania content lower than 20% in molar concentration, the epoxy ring is preserved and some residual mobility is observed in the organic terminal part of GPTMS. When the amount of germania exceeds this limit a significant effect on the epoxy opening was observed, with almost 70% of the epoxy groups that have reacted during the synthesis. The different characterization techniques have been used to obtain a semiquantitative comparative evaluation of the amount of epoxides. ^{13}C CP MAS NMR experiments have shown that the epoxy groups give rise to the formation of short polyethylene species. The residual mobility of GPTMS has allowed the use of NMR techniques initially developed for liquids that have brought a better understanding of the hybrid structure. This has been done, in particular, using indirect scalar couplings $^1J_{C-H}$ for $^1H \rightarrow {}^{13}C$ polarization transfers.

Introduction

Germanium oxides and germanosilicate glasses are very important photonics materials. Several key applications, such as optical fibers are, in fact, based on their optical properties.[1] The refractive index change, induced by ultraviolet light, in germania-containing glass is an important property to fabricate photonic devices, such as Bragg gratings.[2] The low phononic energy of germania is also another interesting property because it can be used to produce low losses optical waveguides and amplifiers.[3] Materials for photonics require a very high level of purity and homogeneity and sol−gel processing is, therefore, an important route to fabricate germania-based materials with advanced and controlled properties.[4]

Sol−gel processing of oxide materials, bulk and thin films, requires however a high firing temperature to achieve a full densification. During this process some oxides show a tendency to crystallize. This is actually the case of several oxides, such as titania, which are used in combination with silica to modulate the refractive index in the preparation of optical waveguides; a high refractive index is, in fact,

* To whom correspondence should be addressed. E-mail: plinio@uniss.it.

(1) Hirai, Y.; Fukuda, T.; Kubota, K. *J. Non-Cryst. Solids* **1987**, *93*, 431.
(2) Hill, K. O.; Fujii, Y.; Johnson, B. S.; Kawasaki, B. S. *Appl. Phys. Lett.* **1978**, *32*, 647.
(3) Brusatin, G.; Guglielmi, M.; Martucci, A. *J. Am. Ceram. Soc.* **1997**, *80*, 3139.
(4) Grandi, S.; Mustarelli, P.; Agnello, S.; Cannas, M.; Canonizzo, A. *J. Sol−Gel Sci. Technol.* **2003**, *26*, 915.

10.1021/cm047765g CCC: $30.25
Published on Web 05/11/2005

necessary to fabricate waveguides based on the "silica on silicon" technology. Germania-based sol−gel materials have been widely investigated as materials for optical waveguides in passive[5] and active devices,[6] such as erbium-doped oxides for light amplification. The easy crystallization of germania at low temperatures represents, however, a difficult problem to solve when sol−gel processing is employed for the fabrication process. Germania sol−gel glasses generally crystallize after firing at temperatures higher than 500 °C and a full densification cannot be achieved without avoiding a partial crystallization of the system.[3] Another related problem is the presence of residual OH groups after processing of sol−gel oxide films. This is a serious limitation to use of the materials in the telecommunication wavelength, because of the optical absorption losses induced by the presence of the residual hydroxyls.

Hybrid materials, on the other hand, have shown the possibility to be densified at low temperatures (∼150 °C) showing, on average, surprisingly low optical propagation losses even in the near-infrared region.[7] Germania hybrids represent, therefore, an interesting material for several photonic applications.

A limitation in a wider application of hybrid materials is, however, the lack of a deeper knowledge and control of their structure. In several cases it was observed that control of the hybrid structure through an appropriate and reproducible synthesis is a difficult task. In this article we present a simple route to synthesize germania-based hybrid materials. We have applied a combination of advanced nuclear magnetic resonance (NMR) techniques and infrared and Raman spectroscopies to obtain a clear understanding of the formation of the structure in germania hybrids synthesized using 3-glycidoxypropyltrimethoxysilane as the organically modified alkoxide. The control of the structure is a critical target because of the simultaneous organic and inorganic polycondensation, through the epoxy opening and the hydrolytic reactions of the alkoxy functionalities.

Experimental Section

Materials. The precursor sol was synthesized employing tetramethoxysilane (TMOS), 3-glycidoxypropyltrimethoxysilane (GPTMS), and tetraethoxygermane (TEOG) as precursors. They were all purchased from Aldrich and used without further purification. Methanol (MeOH) (Aldrich) was employed as solvent, doubly distilled water was used for hydrolysis, and hydrochloric acid (1 N) was used as catalyst.

Synthesis of the Sols. Four different sols were prepared by changing the relative molar ratios of the precursor alkoxides: (1) TEOG/TMOS/GPTMS = 0:30:70 (Ge0T3G7); (2) TEOG/TMOS/GPTMS = 20:10:70 (Ge2T1G7); (3) TEOG/TMOS/GPTMS = 10:20:70 (Ge1T2G7); and (4) TEOG/TMOS/GPTMS = 30:0:70 (Ge3T0G7). Water and the catalyst were added to reach the following final molar ratios in all the sols: (GPTMS + TMOS + TEOG)/HCl = 1:0.008; (GPTMS + TMOS + TEOG)/H_2O = 1:2.

The Ge2T1G7 and Ge1T2G7 sols were prepared in three different steps: in the first one GPTMS was first reacted 1 h at room temperature (H_2O/GPTMS = 2). Immediately afterward, in the second step, MeOH, TEOG, and H_2O, (H_2O/TEOG) = 2, were added in order, and the sol was reacted for another 3 h at room temperature; the ratio (TEOG + GPTMS)/MeOH was 0.15. Separately a solution of MeOH, TMOS, and HCl was prepared, (GPTMS + TMOS + TEOG)/HCl = 1:0.008, stirred for 2 h reaction at room temperature (TMOS/MeOH = 0.05), and then added in the final sol that was left to react for another hour at room temperature. The final oxide concentration in the sol was 100 gL^{-1}.

The sol Ge3T0G7 was prepared following the same protocol of Ge2T3G7 and Ge1T2G7 for the first two steps, but without the final addition of a pre-hydrolyzed silica sol.

The sol Ge0T3G7 was synthesized by adding to a sol of GPTMS and H_2O (GPTMS/H_2O = 2) prehydrolyzed for 1 h at room temperature a silica sol of TMOS and HCl [(GPTMS + TMOS)/HCl = 1: 0.008]. Methanol was added to reach, also in this case, a SiO_2 oxide concentration of 100 gL^{-1}. The final sol was reacted for another 90 min under reflux at 90 °C.

Materials Preparation. Powders were prepared by pouring the sol in glassware and drying it in air in an oven at 60 °C. The dried gel was milled to obtain a fine powder. These powders were analyzed by multinuclear solid-state NMR and vibrational spectroscopies.

NMR Characterization. ^{29}Si MAS NMR spectra were recorded on a MSL400 Bruker spectrometer (ν (^{29}Si) = 79.5 MHz) with a 7-mm CP MAS probe, using 90° pulse duration (6.5 μs) and 100-s recycle delays. The magic angle spinning (MAS) rate ν_{MAS} was 4 kHz.

^{1}H and ^{13}C{^{1}H} NMR spectra were acquired on a Bruker DSX 400 spectrometer (ν(^{1}H) = 400.1 MHz, ν(^{13}C) = 100.6 MHz) with double resonance 2.5- or 4-mm ^{1}H−X MAS probes. MAS rates ν_{MAS} were adjusted from 10 to 35 kHz depending on samples and experiments. The radio frequency field strengths for ^{1}H and ^{13}C pulses were ca. 50 kHz. Simple pulse ^{1}H spectra were obtained with 90° pulse duration and 2-s recycle delays. ^{1}H−^{1}H 2D exchange[8] or double quantum BABA[9] experiments were done using same general parameters. For BABA experiments, excitation and reconversion periods τ_e and τ_r were varied from 62.5 to 375 μs. Single pulse ^{13}C{^{1}H} spectra were obtained with 20° pulse duration and 10-s recycle delays. Continuous ^{1}H decoupling during ^{13}C signal acquisition was employed (same RF field strengths). Contact time τ_c for ^{13}C{^{1}H} cross-polarization (CP) experiments was 2 ms. Pumping and refocusing delays Δ_1 and Δ_2 of the ^{13}C{^{1}H} 2D INEPT experiments[10] were optimized for each sample following previous work.[11]

(5) (a) Chen, D.-G.; Potter, B. G.; Simmons J. H. *J. Non-Cryst. Solids* **1994**, *178*, 135. (b) Jing, C. B.; Zhao, X. J.; Tao, H. Z.; Wang, X. N.; Liu, A. Y. *J. Mater. Chem.* **2003**, *13*, 3066.

(6) (a) Yamazaki, M.; Koijima, K. *J. Mater. Sci. Lett.* **1995**, *14*, 813. (b) Martucci, A.; Chiasera, A.; Montagna, M.; Ferrari, M. *J. Non-Cryst. Solids* **2003**, *322*, 295. (c) Nogami, M. *J. Lumin.* **2001**, *92*, 329. (d) Xiang, Q.; Zhou, Y.; Ooi, B. S.; Lam, Y. L.; Chan, Y. C.; Kam, C. H. *Thin Solid Films* **2000**, *370*, 243. (e) Duverger, C.; Ferrari, M.; Mazzoleni, C.; Montagna; M., Pucker, G.; Turrell, S. *J.Non-Cryst. Solids* **1999**, *245*, 129. (f) Strohhöfer, C.; Capecchi, S.; Fick, J.; Martucci, A.; Brusatin, G.; Guglielmi, M. *Thin Solid Films* **1998**, *326*, 99. (g) Benatsou, M.; Bouazaoui, M. *Opt. Comm.* **1997**, *137*, 143.

(7) (a) Rosh, O. S.; Bernhard, W.; Muler-Fiedler, R.; Danberg, P.; Brauer, A.; Buestrich, R.; Popall, M. *Proc. SPIE−Int. Soc. Opt. Eng.* **1999**, *3799*, 214. (b) Buetrich, R.; Kahlemberg, F.; Popall, M.; Dannberg, P.; Muler-Fiendler, R.; Rosh, O. *J. Sol-Gel Sci. Technol.* **2001**, *20*, 181.

(8) Jeener, J.; Meier, B. H.; Bachmann P.; Ernst, R. R. *J. Chem. Phys.* **1979**, *71*, 4546.

(9) Sommer, W.; Gottwald, J.; Demco, D. E.; Spiess, H. W. *J. Magn. Reson.* **1995**, A *113*, 131.

(10) (a) Morris, G. A.; Freeman, R. *J. Am. Chem. Soc.* **1979**, *101*, 760. (b) Burum, D. P.; Ernst, R. R. *J. Magn. Reson.* **1980**, *39*, 163. (c) Bax, A.; Morris, G. A. *J. Magn. Reson.* **1981**, *42*, 501.

(11) Alonso, B.; Massiot, D. *J. Magn. Reson.* **2003**, *163*, 347.

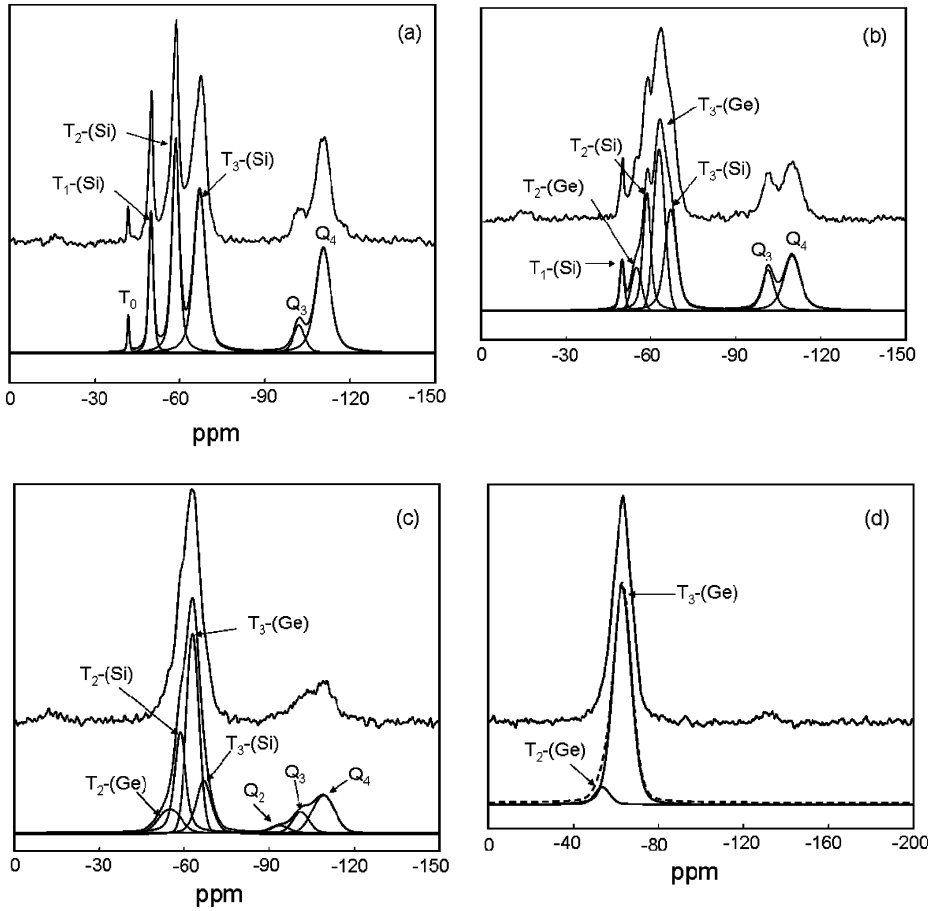

Figure 1. ^{29}Si MAS NMR solid-state spectra of (a) Ge0T3G7, (b) Ge1T2G7, (c) Ge2T1G7, and (d) Ge3T0G7. The measured spectra are shown in the upper part of the figures, the deconvoluted spectra are shown in the lower part.

^{1}H, ^{13}C, and ^{29}Si chemical shift referencing is relative to external TMS. Deconvolutions of the spectra were done using the DmFit2003 Program.[12]

FTIR Characterization. Infrared absorption spectra in the range 4500−400 cm^{-1} were recorded by Fourier transform infrared spectroscopy (FTIR) (Perkin-Elmer 2000), with a resolution of ±1 cm^{-1}, 256 scans. The spectra were recorded in transmission using KBr to prepare thin disks with the sample powder. A Gaussian peak fitting procedure has been applied to the FTIR spectra (Microcal Origin Software), the quality of the fitting was evaluated on the basis of the χ^2-values (in the order of 10^{-6}) and correlation coefficient values ≥0.998. C−H stretching at 2875 cm^{-1} was used to normalize the spectra.

FT-Raman Analysis. The Raman spectra were recorded by a JUSCO spectrometer, using the 1064-nm line of a Nd:YAG laser generating the power of 250 mW on the sample and a spectral resolution of 4 cm^{-1}. The C−H deformation band at 1456 cm^{-1} was used to normalize the spectra.

Results and Discussion

Formation of the Inorganic Network. The preparation of mixed oxide hybrid materials, with a covalent bonding between the organic and inorganic networks (Class II hybrids), such as SiO_2-TiO_2 or SiO_2-ZrO_2, generally requires a very careful control of the conditions of synthesis.[13] The possibility to achieve a homogeneous material requires, in fact, hydrolytically stable mixed bonds,[14] which are, for instance, quite critical to obtain in SiO_2-TiO_2 hybrids,[15,16] and a homogeneous distribution of the oxides within the hybrid network, without phase separation.[17]

Figure 1 shows the ^{29}Si MAS NMR spectra of the different samples after drying at 60 °C. These are the standard preparation conditions that were used for the hybrid powders. The spectra have been deconvoluted and the results are also reported in Figure 1.

The spectrum of Ge0T3G7 (Figure 1a) presents two families of resonances assigned to Q units (peaks at −102.1 and −110.6 ppm) and T units (peaks at −41.8, −49.9, −58.6 and −67.0 ppm). These units come from the hydrolysis of TMOS and GPTMS respectively, and have been assigned to Q_3 and Q_4, and T_0, T_1, T_2, and T_3. Their relative percentages are reported in Table 1. One can notice the high extent of condensation of the Q units (96%), compared to the T units (76%), for which even unhydrolyzed units are still present. Also, the peaks of the T units are quite narrow,

(12) A shareware version of the Program can be downloaded at http://crmht-europe.cnrs-orleans.fr.

(13) Innocenzi, P.; Brusatin, G.; Guglielmi, M.; Bertani, R. *Chem. Mater.* **1999**, *11*, 1672.

(14) Hoebbel, D.; Nacken, M.; Schmidt, H. *J. Sol−Gel Sci. Technol.* **2001**, *21*, 177.

(15) (a) Hoebbel, D.; Nacken, M.; Schmidt, H. *J. Sol−Gel Sci. Technol.* **1998**, *12*, 169. (b) Hoebbel, D.; Nacken, M.; Schmidt, H. *J. Sol−Gel Sci. Technol.* **1998**, *13*, 37. (c) Gervais, C.; Babonneau, F.; Hoebbel, D.; Smith, M. E. *Sol. State Nucl. Magn. Res.* **2000**, *17*, 2.

(16) Crouzet, L.; Leclercq, D.; Mutin, H. P.; Vioux, A. *Chem. Mater.* **2003**, *15*, 1530.

(17) Babonneau, F.; Maquet, J. *Polyhedron* **2000**, *19*, 315.

Table 1. Chemical Shifts Assignment of the Bands Resolved from the Deconvolution of the ^{29}Si MAS NMR Spectra of the Hybrid Samples

sample	composition	chemical shift (ppm)	%[a]	assignment	degree of condensation (%)
Ge3T0G7	Ge:Si:GPTMS = 30:0:70	−63.1	94	T_3: $RSi(OGe...)_{3-n}(OSi...)_n$ {$n < 3$}	
		−53.8	6	T_2: $RSi(OGe...)_{2-n}(OSi...)_n(OX)$ {$n < 1$, X≡H, Me, or Et}	
Ge2T1G7	Ge:Si:GPTMS = 20:10:70	−109.1	12	Q_4	
		−101.1	5	Q_3	
		−93.7	2	Q_2	88
		−67.0	15	T_3: $RSi(OSi...)_3$	
		−63.0	37	T_3: $RSi(OGe...)_{3-n}(OSi...)_n$ {$n < 3$}	
		−58.6	21	T_2: $RSi(OSi...)_2(OX)$ {X≡H, Me, or Et}	
		−54.9	8	T_2: $RSi(OGe...)_{2-n}(OSi...)_n(OX)$ {$n < 1$, X≡H, Me, or Et}	88
Ge1T2 G7	Ge:Si:GPTMS = 10:20:70	−109.8	16	Q_4	
		−101.4	9	Q_3	91
		−67.0	21	T_3: $RSi(OSi...)_3$	
		−63.0	27	T_3: $RSi(OGe...)_{3-n}(OSi...)_n$ {$n < 3$}	
		−58.6	17	T_2: $RSi(OSi...)_2(OX)$ {X≡H, Me, or Et}	
		−54.9	6	T_2: $RSi(OGe...)_{2-n}(OSi...)_n(OX)$ {$n < 1$, X≡H, Me, or Et}	
		−49.9	4	T_1: $RSi(OSi...)(OX)_2$ {X≡H, Me, or Et}	86
Ge0T3G7	Ge:Si:GPTMS = 0:30:70	−110.6	26	Q_4	
		−102.1	5	Q_3	96
		−67.0	31	T_3: $RSi(OSi...)_3$	
		−58.6	27	T_2: $RSi(OSi...)_2(OX)$ {X≡H or Me}	
		−49.9	10	T_1: $RSi(OSi...)(OX)_2$ {X≡H or Me}	
		−41.8	1	T_0: $RSi(OX)_3$ {X≡H or Me}	76

[a] Relative amounts (%) of the different T_n and Q_n species are listed in the fourth column.

suggesting a certain level of mobility in the hybrid network and/or a narrow distribution of environments. These observations should be related to a nanometric phase-separation between rich in T units domains, which are less condensed, and rich in Q units domains. The prehydrolysis of Q units makes these units much more condensed, especially because there is not a significant excess of water to allow a higher extent of condensation for the T units. This local organization is favored by prehydrolyzing TEOS during the synthesis. Also for this sample, all the oxo chemical bonds are siloxane Si−O−Si bonds. Therefore, the ^{29}Si chemical shifts of T_x or Q_y units correspond to that of T or Q units bound respectively to *x* or *y* silicon atoms (Table 1).

The spectrum of Ge3T0G7 (Figure 1d) shows only one broad peak due to T units that can be deconvoluted into two signals located at −53.8 and −63.1 ppm, and tentatively assigned to T_2 and T_3 units. Peak line widths are much broader for this sample, suggesting the existence of a wide distribution of environments. Indeed, the observed shift of the peaks compared to the previous spectrum strongly suggests the presence of Si−O−Ge bonds.

The spectra of Ge1T2G7 and Ge2T1G7, samples based on three precursors, TEOG, TMOS, and GPTMS, have been compared to the two previous samples (Figure 1b and c). The peaks due to the Q units have slightly shifted, with the increasing amount of Ge, and this could be related to the formation of bonds between SiO_2 and GeO_2 tetrahedra. But the main influence of the introduction of Ge can be seen by looking at the T units signals. The deconvolution reveals the presence of overlapped signals: one series corresponding to signals found in Ge0T3G7 and another series of signals similar to those found in Ge3T0G7 (Table 1). The first series would correspond to T units only bound to silicon atoms, and the second series would correspond to T units bound to at least one germanium. A homogeneous distribution of SiO_2 and GeO_2 tetrahedra within the hybrid network should lead to a single distribution of chemical shifts, which is not exactly observed. We remark that increasing the amount of Ge, the percentage of T units only bounded to silicon atoms strongly decrease. For the sample Ge3T0G7, these percentages are close to zero when they should be close to 2% for $RSi(OSi...)_2(OX)$ and to 24% for $RSi(OSi...)_3$ in the case of a random distribution of units.[18] It is likely the T units are preferentially bound to GeO_2 tetrahedra rather than other T units. The comparison among the 4 samples confirms the important role of the presence of Ge on the extent of condensation of the T units from GPTMS (Table 1). A reverse behavior, but on a minor scale, is observed for Q units: this could show that Ge is preferentially bonded to T units rather than Q units.

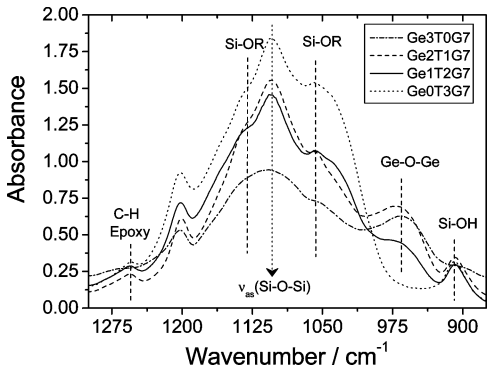

Figure 2. FTIR absorption spectra of the samples prepared with different amounts of germania in the 1250−875 cm^{-1} range.

Figure 2 shows the FTIR absorption spectra in the 1250−875 cm^{-1} range. In this interval the main Si−O−Si symmetric stretching mode (∼1100 cm^{-1}), is observed in silica containing samples.[19] This band increases in intensity with

(18) Supplementary Information 1 (in the Supporting Information) is a Table to compare the percentages corresponding to a random distribution of units with the experimental ones.

(19) Innocenzi, P. *J. Non-Cryst. Solids* **2003**, *316*, 309.

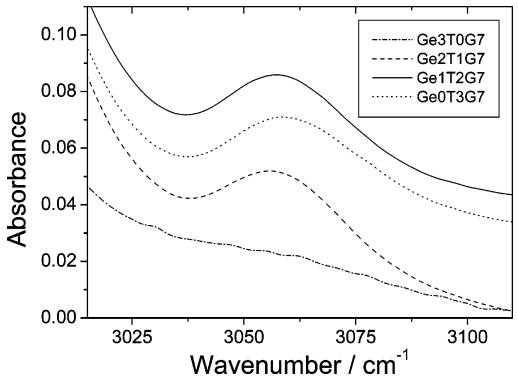

Figure 3. FTIR absorption spectra of the samples prepared with different amounts of germania around 3060 cm^{-1} (C−H epoxy stretching).

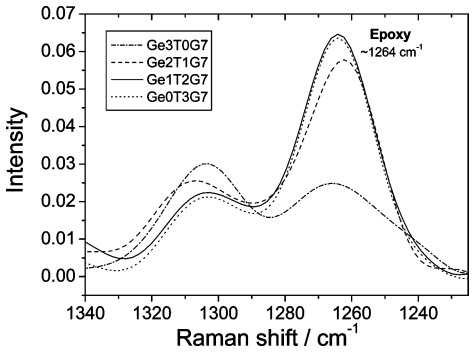

Figure 4. FT-Raman normalized spectra of the samples prepared with different amounts of germania.

the decrease of GeO_2 content in the samples. Lower amounts of GeO_2, on the other hand, increase the intensity of the shoulders at 1060 and 1130 cm^{-1} due to the presence of unreacted Si−OR groups. The effect of Ge is also reflected by the change in intensity of the 1260 cm^{-1} (epoxy ring) and 970 cm^{-1} band (Ge−O−Ge).[20] The Si−OH band decreases in intensity in the samples with higher GeO_2 contents, supporting the observations from ^{29}Si NMR spectra that higher amounts of TEOG are also effective to catalyze the condensation of silicon alkoxides.

Ring Opening in the Epoxies Studied by FTIR and FT-Raman. An indication of the opening degree of the epoxy ring in the solid state can be obtained by infrared and Raman spectroscopies. These techniques can be employed for a semiquantitative evaluation of the epoxy ring opening without obtaining, however, any direct information on the extent of the polymerization reactions. Other information, concerning the inorganic network condensation and the formation of mixed Si−O−Ge oxide bonds, could also be obtained.

In the middle infrared range, the epoxy ring in GPTMS has four characteristic vibrational modes:[21] at 1260−1240 cm^{-1} (ring breathing), 950−810 cm^{-1} (antysimmetric ring stretching), 865−785 cm^{-1} (unassigned), and 3050−2995 cm^{-1} due to C−H stretching. The antisymmetric ring stretching mode (∼900 cm^{-1}) is generally chosen in epoxy resins to evaluate ring opening in hybrid materials. However, this band overlaps with the Si−OH stretching band and the 3050 cm^{-1} mode seems more representative. Figure 3 shows the FTIR absorption spectra of the hybrid samples in the range 3015−3110 cm^{-1}. It can be observed that only an amount of Ge/Si molar ratio higher than 20% catalyzes the opening reaction of the epoxy ring, in accordance with ^{13}C NMR (vide infra). In the Ge3T0G7 sample around 86% of the epoxy groups have reacted. This evaluation was done using the difference in the relative absorption intensities with respect to Ge0T3G7. There is, however, a certain degree of uncertainty due to the choice of the reference baseline that is likely overestimating the amount of reacted epoxy rings. If, instead, the integrated area of the band due to the epoxy groups (which needs a different choice of the baseline) is used, the calculated amount of reacted groups decreases down to 64%.

The epoxy ring shows also characteristic Raman bands[22] at 842−852 cm^{-1} (epoxy symmetric deformation), 908 cm^{-1} (epoxy antisymmetric deformation), 1135 cm^{-1} (epoxy CH_2 wagging), 1256 cm^{-1} (epoxy ring breathing), 1414 cm^{-1} (epoxy CH_2 twisting), and 1478 cm^{-1} (epoxy CH_2 bending). The 1256 cm^{-1} band is generally quite intense and is chosen to follow the reactions of the epoxy rings,[23] in our material, this band is located at 1264 cm^{-1}. Figure 4 shows the FT-Raman spectra in the range 1225−1340 cm^{-1}, the trend observed is well in accordance to the results found from FTIR spectra (Figure 3): the epoxy bands decrease with an increase in the Ge content of the samples.

^{13}C CP MAS NMR Spectra. Another important feature concerning the structural control in hybrid materials is related to the formation of the organic network. Employing organically modified alkoxides bearing polymerizable organic functionalities, such as epoxy or methacryloxy, has in fact a direct influence on the final structure.[24] Several complex chemical processes are involved in the formation of the hybrid structure, and the different rates of the organic and inorganic polycondensations mutually affect the formation of the hybrid network. To understand the extent of polycondensation and the type of organic moieties formed from the reaction of the epoxy groups (in the case of GPTMS-based hybrids), ^{13}C NMR is an important tool.

Figure 5 shows the ^{13}C CP MAS NMR spectra of the hybrid materials after drying at 60 °C. Spectra of samples Ge0T1G7, G1T2G7, and Ge2T1G7 are practically identical with the exception of the presence of residual methoxy groups around 50 ppm. In contrast, the Ge3T0G7 spectrum shows marked differences. The ^{13}C chemical shifts obtained through CP are listed in Tables 2 and 3, respectively, for samples Ge0T1G7 and Ge3T0G7. The assignments, made on the basis of our previous works[13,24] (see supplementary information 2 in the Supporting Information) and litera-

(20) Lipinska-Kalita, K. E. *J. Non-Cryst. Solids* **1990**, *119*, 41.
(21) *Atlas of Spectral Data and Physical Constants for Organic, Compounds*; Grasselli, J. G., Ritchey, W. M., Eds.; CRC Press Inc.: Cleveland, OH, 1975; Vol. I.
(22) (a) Posset, U.; Lankers M.; Kiefer, W.; Steins, H.; Schottner G. *Appl. Spectrosc.* **1993**, *47*, 1600. (b) Riegel, B.; Kiefer, W.; Hofacker, S.; Schottner G. *J. Sol−Gel Sci. Technol.* **2002**, *24*, 139.
(23) Riegel, B.; Blittersdorf, S.; Kiefer, W.; Hofacker, S.; Muller, M., Schottner G. *J. Non-Cryst. Solids* **1998**, *226*, 76.
(24) (a) Innocenzi, P.; Brusatin, G.; Babonneau, F. *Chem. Mater.* **2000**, *12*, 3726. (b) Innocenzi, P.; Brusatin, G.; Licoccia, S.; Di Vona, M.; Babonneau, F.; Alonso, B. *Chem. Mater.* **2003**, *15*, 4790. (c) Davis, S.; Brough, A. R.; Atkinson, A. *J. Non-Cryst. Solids* **2003**, *315*, 197. (d) Templin, M.; Wiesner, U.; Spiess, H. W. *Adv. Mater.* **1997**, *9*, 814.

Table 2. ^{1}H and ^{13}C NMR Data Based on ^{1}H Fast MAS, ^{1}H−^{13}C 2D INEPT, ^{13}C{^{1}H} CP, and ^{1}H−^{1}H BABA Experiments for the Sample Ge0T3G7

^{1}H fast MAS		^{1}H−^{13}C 2D INEPT		^{13}C{^{1}H} CP		nearest protons
δ(^{1}H) (ppm)	area (%)	δ(^{1}H) (ppm)	δ(^{13}C) (ppm)	δ(^{13}C) (ppm)	assignment	^{1}H−^{1}H BABA
0.74	4.5	0.73	∼8	∼10	1	3−5−6_{anti}−6_{syn}
0.79	15.1			∼10	1 (broad contribution)	
1.27	0.3				Si**O**H	
1.76	14.1	1.76	23.7	24	2	3−4_a−4_b−5−6_{anti}−6_{syn}
2.60	7.9	2.59	44.3	45	6_{anti}	1−2−4_a−6_{syn}
2.79	7.6	2.78	44.3	45	6_{syn}	1−2−3−5−4_b−6_{anti}
3.14	7.7	3.13	51.3	52	5	1−2−3−4_a−6_{syn}
3.41	13.8	3.39	72.0	73	4_a	2−4_b−5−6_{anti}−6_{syn}
		3.45	50.2	∼50	C**H**$_3$−OSi(O...)$_2$(CH_2-...)	
3.52	5.4	3.52	73.9	75	3	1−2−5−6_{syn}
3.59	4.8	3.62	50.5	∼50	C**H**$_3$−OSi(O...)$_3$	
3.71	18.9	3.71	72.0	73	4_b	2−4_a−5−6_{anti}−6_{syn}

ture[25,26] and supported by ^{1}H experiments (vide infra), are shown in Scheme 1 relative to GPTMS.

The sharpness of the peaks around 73 and 75 ppm (positions 3 and 4, respectively) reveals that in all the samples, with the exception of Ge3T0G7, the carbon atoms of the ether bridge are in a well-defined site (no chemical shift dispersion) and in a mobile chain (long transverse relaxation times are presumed). In addition, for sample Ge3T0G7, the signals at 52 and 45 ppm of carbons in the epoxy rings (5 and 6, respectively) strongly decrease in intensity. Also, the two carbon atoms closer to silicon, whose peaks are observed at 10 and 24 ppm, show a relative broadening of the signal in Ge3T0G7, with the increased siloxane network rigidity due to the completion of the organic and inorganic polycondensation reactions. Moreover, in Ge3T0G7 a broad peak around 70−75 ppm, formed by the superimposition of peaks obtained after the epoxy opening, is observed. This is an indication that the addition of TEOG catalyzes the epoxy opening only for Ge/Si molar ratios larger than 20%. The sharpness of the overlapped peaks is also an indication that these species are relatively mobile.

Chain Conformations from ^{1}H and ^{13}C NMR Data. The description of the conformation and/or the localization of organic groups in hybrid materials can give some important indications on the synthesis process and on the final network. Recent solid-state NMR developments, such as fast MAS,

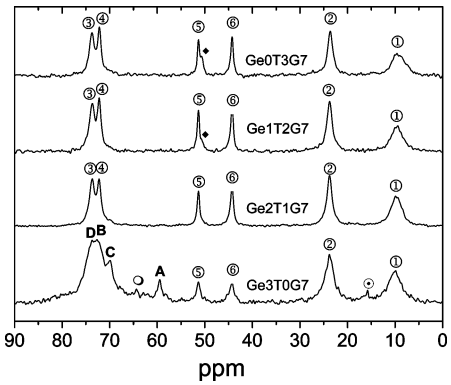

Figure 5. ^{13}C CP MAS NMR spectra of the samples prepared with different amounts of germania. The attributions of the different chemical shifts are listed in Table 2. The numbers in the figure are referred to carbon atoms as labeled in Scheme 1: A = terminal methyl ether group (−O−CH_2−C(OH)−CH_2−O-***C***H_3); B, C, D = carbons in the poly(ethylene oxide) chain (−O−CH_2−[−***C***H_2−***C***H_2−]$_n$−O−); ⊙ carbons in residual ethoxy groups (−O−***C***H_2−CH_3); ◆ Carbons in residual methanol or methoxy groups (Si−O***C***H_3 ; H−O***C***H_3).

Scheme 1

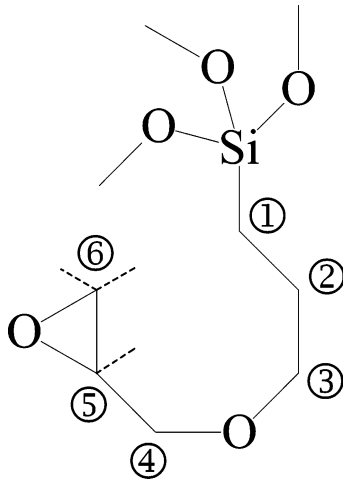

allow increasing the resolution in ^{1}H spectra, and hence using this resolution for studying spatial proximities between organic groups. For these reasons, ^{1}H NMR is becoming a powerful tool for the analysis of hybrid materials.[27]

^{1}H fast MAS NMR spectrum of Ge0T3G7 is shown in Figure 6a, with its deconvolution in Figure 6b. The area of each deconvoluted peak is proportional to the abundance of each type of protons. The two inequivalent protons bonded to the carbon in position 6 (see Scheme 1) give sharp and intense signals in positions 2.60 ppm (6_{anti}) and 2.79 ppm (6_{syn}). Therefore, in accordance with ^{13}C CP data (vide supra), the epoxy ring in this sample is preserved and no polymerization occurs. The "glycidyl" groups can thus conserve some residual mobility that contributes to the sharpness of ^{1}H and ^{13}C signals. The combination of this mobility with fast MAS allows using a "palette" of NMR methods initially developed for liquids, and especially to correlate the ^{13}C signals to that of ^{1}H by using indirect scalar couplings $^1J_{C-H}$ for ^{1}H→^{13}C polarization transfers.[11] The two-dimensional (2D) correlation through an INEPT experiment is shown in Figure 7a. Signal

(25) Lee, T.-H.; Kang, E.-S.; Bae, B.-S. *J. Sol-Gel Sci. Technol*. **2003**, *27*, 23.
(26) Davis, S. R.; Brough, A. R.; Atkinson, A. *J. Non-Cryst. Solids* **2003**, *315*, 197.
(27) (a) De Paul, S. M.; Zwanziger, J. W.; Ulrich, R.; Wiesner, U.; Spiess, H. W. *J. Am. Chem. Soc*. **1999**, *121*, 5727. (b) Massiot, D.; Alonso, B.; Fayon, F.; Fredoueil, F.; Bujoli, B. *Solid State Sci*. **2001**, *3*, 11. (c) Alonso, B.; Fayon, F.; Fredoueil, F.; Bujoli, B.; Massiot, D. *J. Sol-Gel Sci. Technol*. **2003**, *26*, 95. (d) Camus, L.; Goletto, V.; Maquet, J.; Gervais, C.; Bonhomme, C.; Babonneau, F.; Massiot, D. *J. Sol-Gel Sci. Technol*. **2003**, *26*, 311.

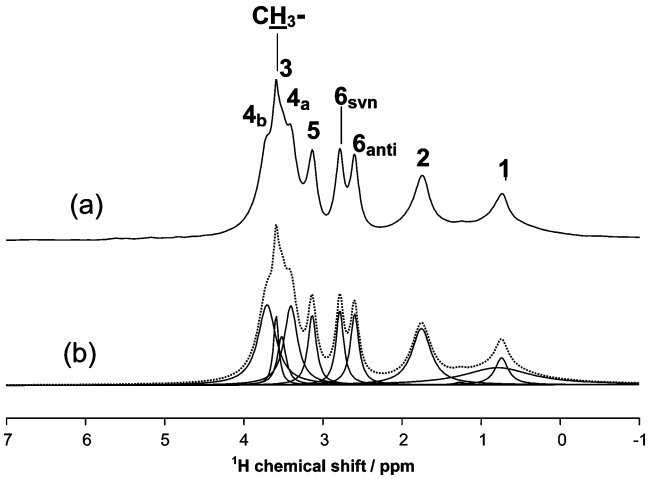

Figure 6. (a) ^{1}H fast MAS NMR spectra of Ge0T3G7 (2.5-mm rotor probe, $\nu_{MAS} = 32$ kHz, 4 scans); (b) corresponding deconvolution.

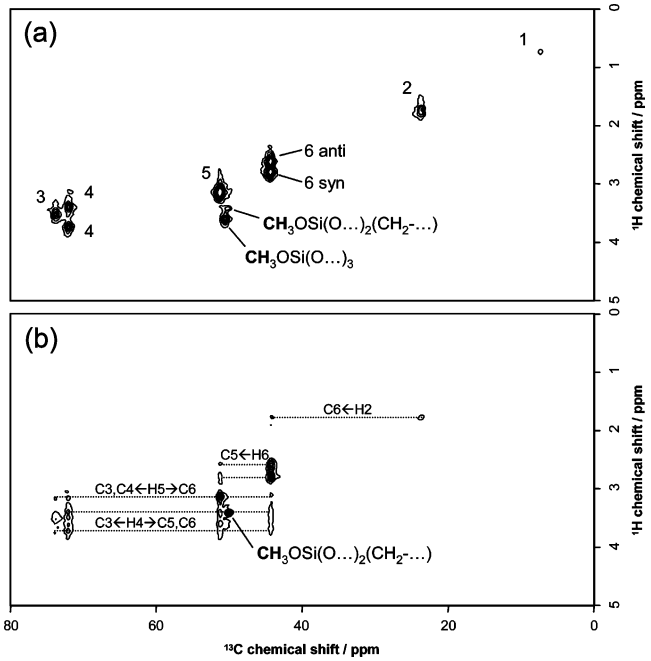

Figure 7. (a) ^{1}H−^{13}C 2D INEPT spectrum for Ge0T3G7 (2.5-mm rotor probe, $\nu_{MAS} = 32$ kHz, $\Delta_1 = 1.1$ ms, $\Delta_2 = 0.8$ ms, 32 scans, 1024 × 256 data points); (b) ^{1}H−^{13}C 2D INEPT spectrum for Ge0T3G7 with a ^{1}H mixing time $\tau_m = 62.5$ ms (2.5-mm rotor probe, $\nu_{MAS} = 32$ kHz, $\Delta_1 = 1.1$ ms, $\Delta_2 = 0.8$ ms, 64 scans, 1024 × 256 data points).

intensities depend here on both $^1J_{C-H}$ and the effective transverse relaxation times T_2, very sensitive to averaged dipolar couplings and residual mobility. From this 2D correlation and from literature data,[28] ^{1}H and ^{13}C signals of the organic groups are unambiguously assigned (Table 2). It is noticeable that for this sample, inequivalent protons of methylene groups can be distinguished as in liquid-state NMR.[28]

Various NMR methods can be used to spatially localize the organic groups. For example, a mixing time τ_m can be included in the INEPT experiment to explore the spatial proximities between ^{1}H−^{13}C pairs.[11] During τ_m, ^{1}H NOE or spin diffusion processes (respectively, for mobile or rigid systems) are introduced. Therefore, polarization can be exchanged and relayed between protons coupled by dipolar or residual dipolar interactions. The mixing time τ_m during which this exchange occurs will determine the range of distances explored. Figure 7b represents the 2D spectrum obtained with $\tau_m = 62.5$ ms. New correlation peaks between signals of the glycidyl group are noticed (^{1}H, ^{13}C at positions 4, 5, and 6). In addition, protons in positions 4 and 5 correlate with that of position 3, and protons in position 2 correlate with that of position 6. These new correlations suggest that the organic chain adopts a "curved" conformation similar to that evidenced using liquid-state NMR.[28] A series of ^{1}H−^{1}H exchange 2D experiments run at various mixing times ($0 < \tau_m < 500$ ms) was recorded (not shown). We observed several new off-diagonal correlation peaks. The resulting diffusion curves (normalized intensities as a function of τ_m) are very similar. This reveals a nearly homogeneous multispin system at the nanometer scale. In that sense, no specific organization of the organic chains between them can be suspected.

More information on spatial proximities is deduced from double-quantum experiments based on homonuclear dipolar couplings. For that purpose, the BABA scheme[9] under fast MAS can be satisfactorily implemented.[29] Signal intensities in ^{1}H−^{1}H BABA 2D correlations depend on the strength of the dipolar couplings. In the ideal case of pairs of nuclei, the dipolar couplings depend on the internuclear distances, and might reveal the precise conformation of organic moieties. For nonrigid compounds, however, dipolar couplings are also scaled as a function of the molecular motion. If the distance between two nuclei is fixed and known (e.g., in a phenyl ring), it could be possible to deduce an order parameter that defines the degree of motion.[30] In our case, the distances between protons, as well as the molecular motion are not known. However, it is possible to evidence qualitatively some spatial proximities. We have to keep in mind that dipolar couplings between protons located on a single mobile glycidyl group (intramolecular) will be higher than dipolar couplings between protons located on different mobile glycidyl groups (intermolecular). (The full set of 1D BABA and 2D BABA experiments, where only reconversion and excitation times are varied, are shown in Supplementary Information 3 in the Supporting Information). Figure 8 represents one of the 2D spectra obtained. The detected pairs reveal the spatial proximities, which are reported in Table 2. (The smallest correlation peaks not observed in Figure 8 are shown in Supplementary Information 4). The proximities between protons in positions 5, 6 and protons in positions 1, 2, as well as the absence of correlation between signal 1 and signals 2 and 4, confirm a "bent" conformation.[30]

Formation of a Rigid Hybrid Network. The addition of TEOG in the sol favors, as observed by FTIR, FT-Raman, and ^{13}CP MAS NMR, the epoxy ring opening. This ring opening may result in a polycondensation that will rigidify the hybrid network. It can be, therefore, more clearly

(28) Innocenzi, P.; Sassi, A.; Brusatin, G.; Guglielmi, M.; Favretto, D.; Bertani, R.; Venzo, A.; Babonneau, F. *Chem. Mater.* **2001**, *13*, 3635.

(29) Schnell, I.; Spiess, H. W. *J. Magn. Reson.* **2001**, *151*, 153.

(30) In principle, it could even be possible to differentiate the spatial environment for each proton of the methylene group in position 4. Some additional NMR work is currently being undertaken in this direction.

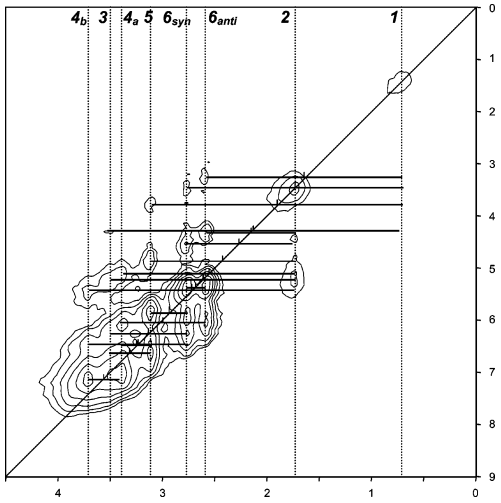

Figure 8. ^{1}H−^{1}H BABA 2D correlations NMR solid-state spectra for Ge0T3G7 (2.5-mm rotor probe, ν_{MAS} = 34 kHz, $\tau_e = \tau_r$ = 250 μs, 16 scans, 1024 × 256 data points).

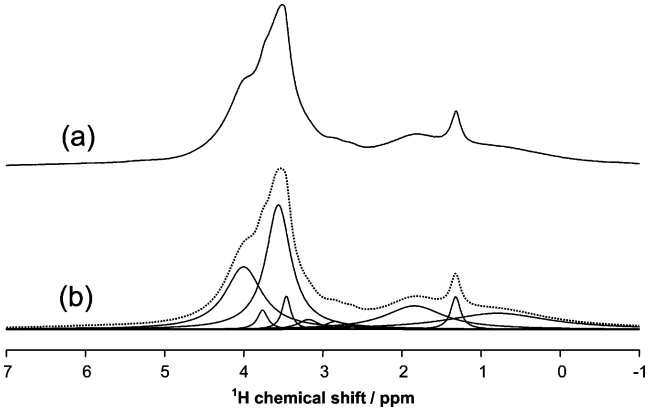

Figure 9. (a) ^{1}H fast MAS NMR spectra of Ge3T0G7 (2.5-mm rotor probe, ν_{MAS} = 34 kHz, 4 scans); (b) corresponding deconvolution.

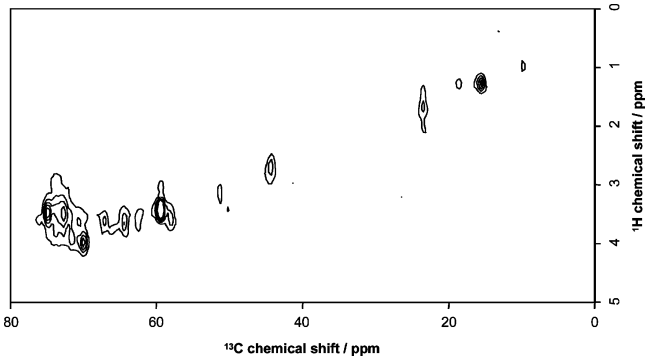

Figure 10. ^{1}H−^{13}C 2D INEPT spectrum for Ge3T0G7 (2.5-mm rotor probe, ν_{MAS} = 34 kHz, $\Delta_1 = \Delta_2$ = 0.6 ms, 192 scans, 1024 × 256 data points).

observed in the sample with the highest amount of germanium, Ge3T0G7, whose ^{1}H fast MAS NMR spectra are shown in Figure 9. A comparison with the corresponding ^{1}H spectra from Ge0T3G7 shows that the signals are now much broader, indicating a significant reduced mobility, while the peaks assigned to protons bonded to epoxy (2.60 and 2.79 ppm) are now only weakly observed as broad overlapped signals.

It was possible to record a ^{1}H−^{13}C INEPT correlation spectrum using fast MAS (Figure 10). The observed peaks are mainly due to the groups still having some residual

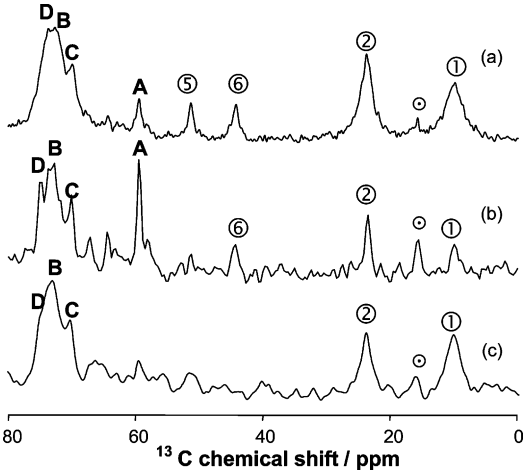

Figure 11. Comparison of ^{13}C{^{1}H} CP, INEPT, and simple pulse spectra NMR spectra for Ge3T0G7; (a) CP (4-mm rotor probe, ν_{MAS} = 11 kHz, τ_c = 2 ms, 1024 scans); (b) INEPT (2.5-mm rotor probe, ν_{MAS} = 34 kHz, $\Delta_1 = \Delta_2$ = 0.6 ms, 192 scans); (c) simple pulse (2.5-mm rotor probe, ν_{MAS} = 34 kHz, 870 scans). The numbers in the figure are referred to carbon atoms as labeled in Scheme 1; ⊙ carbons in residual ethoxy groups (−O−***C***H$_2$−CH$_3$); A = terminal methyl ether group (−O−CH$_2$−C(OH)−CH$_2$−O−***C***H$_3$); B, C, D = carbons in the poly(ethylene oxide) chain (−O−CH$_2$−[−***C***H$_2$−***C***H$_2$−]$_n$−O−).

Table 3. ^{1}H and ^{13}C NMR Data Based on ^{1}H Fast MAS, ^{1}H−^{13}C 2D INEPT, and ^{13}C{^{1}H} CP Experiments for the Sample Ge3T0G7

^{1}H fast MAS		^{1}H-^{13}C 2D INEPT	^{13}C{^{1}H} CP		Assignment
δ(^{1}H) (ppm)	Area (%)	δ(^{1}H) (ppm)	δ(^{13}C) (ppm)		
0.8	15.0	-	-		1
-	-	1.0	10	10	C**H**$_3$-CH$_2$-C
1.3	3.4	1.3	15.7	16	C**H**$_3$-CH$_2$-O-C
		1.3	18.7	16	C**H**$_3$-CH$_2$-O-(H or Si)
1.8	14.0	1.7	23.6	24	2
2.6	0.8	2.7	44.5	45	6_{anti}
2.8	1.8				6_{syn}
3.2	2.2	3.1	51.4	52	5
3.5	3.1	3.5	59.5	59	C**H**$_3$-O-C
		3.5	75.0	~75	C-O-C**H**(-H or R)-CH$_2$
		3.5	71.9	~73	C-O-C**H**$_2$-CH(-H or R)-O
3.6	32.6	3.6	58.2	-	CH$_3$-C**H**$_2$-O-H
		3.6	62.6	65	CH$_3$-C**H**$_2$-O-Si
		3.6	67.2	-	C-C**H**$_2$-O-C
		3.6	70.2	~70	C-O-C**H**$_2$-CH(-H or R)-O
		3.6	72.9	~73	C-O-C**H**$_2$-CH(-H or R)-O
		3.7	64.5	-	C-CH(-H, O or R)-C**H**$_2$-O-H
3.8	2.1	3.8	73.8	~75	C-C**H**(OH)-C
		3.9	71.9	~73	C-C**H**(-OH or OR)-C
4.0	23.8	4.0	70.2	~70	C-C**H**(-OH or OR)-C
5.9	1.3	-	-	-	O**H**

mobility. In that sense, INEPT experiments are complementary to CP experiments.[31] As an example, ^{13}C{^{1}H} CP, INEPT, and simple pulse spectra are compared in Figure 11. ^{1}H and ^{13}C signals are tentatively assigned from the 2D correlation experiments and from literature data (see supplementary information 5) (Table 3). The residual mobility in GPTMS deduced from the INEPT experiments is associated with the terminal parts of the molecule. The two carbon atoms close to silicon and the carbon in position 6 in the epoxy ring result, in fact, still mobile after the polycondensation reactions. The species formed after ring opening, the methyl ether terminal groups, and the oligomers formed after polycondensation of the epoxy ring result also mobile. The mobility of these groups supports the indication from ^{13}C CP MAS spectra (Figure 2) and Figure 11 that short ethylene

(31) Warschawski, D. E.; Devaux, P. F. *J. Magn. Reson.* **2000**, *145*, 367.

Table 4. Comparison of the Epoxy Opening Degree (As Percentage of Epoxy Opened) as a Function of the Germania Content, Measured by Different Techniques

sample	concn of GeO_2 (%)	^{13}C NMR	^{1}H NMR	FT-Raman	FTIR[a]
Ge3T0G7	30	61	88	58	64 86
Ge2T1G7	20	0		9	0
Ge1T2G7	10	0		1	0
Ge0T3G7	0	0	0	0	0

[a] The different values from FTIR are obtained by applying deconvolution methods (64%) or using the relative intensity of the 3050 cm^{-1} band.

oxide chains are formed at different length, upon reaction of the epoxy (vide infra).

From the assignment made in Table 3, the process of epoxy ring opening can be understood as the superposition of a polymerization process and of an "alkoxy ending process". From the precursors and solvents employed, the alkoxy ending groups are both methoxy and ethoxy. Because of the polymerization and the subsequent loss of mobility, and because of the multiplicity of lines, the resolution of the proton spectrum is low. However, the quantification of the residual peaks of the protons in 5 and 6 positions leads to a percentage of ring opening around 88%.

In Table 4 a comparison of the epoxy ring opening evaluated by the three different techniques is shown. The calculated values are quite well in agreement, even if FT-Raman seems more sensitive to evaluate little differences in the epoxy amount. The results show that there is an "on−off" behavior as a function of the GeO_2 concentration. Ge/Si molar ratios as high as 20% will change the material properties (refractive index, defects) without affecting the organic part of the hybrid material through the opening of the epoxy in GPTMS. In the case of NMR, the data from ^{1}H spectra are overestimating the epoxy ring percentage with respect to the other techniques. This is likely related to the fact that the ^{1}H spectra are formed by several overlapped bands, whose deconvolution introduces a certain degree of uncertainty.

Conclusions

Silica−germania hybrid materials have been prepared by 3-glycidoxypropyltrimethoxysilane and tetraethoxygermane. The concentration of germania employed in the synthesis is an important parameter because it can modulate the opening of the epoxy ring; an on−off behavior is observed when the amount of germania exceeds 30% with respect to silica in the samples. In the samples where the epoxy ring is preserved, the terminal part of the organic chain in GPTMS shows a residual mobility. A combination of advanced NMR techniques and infrared and Raman spectroscopies has shown to be very effective in a structural investigation of this class of hybrids. In this case, the NMR techniques, initially developed for liquids, can be applied to study in detail the molecular conformation in the hybrid network. In particular, for this purpose, correlations of ^{13}C signals with that of ^{1}H, by using indirect scalar couplings $^{1}J_{C-H}$ for $^{1}H \rightarrow {}^{13}C$ polarization transfer, has been revealed be very effective to investigate the hybrid structure. A "bent" conformation of GPTMS has been deduced, similar to that in the liquid state. The mobility of the organic chains is lost when epoxy rings are opened to form mainly short ethylene oxide chains, while ^{29}Si NMR spectra suggested that Si−O−Ge mixed bonds are formed.

The resulting two-dimensional $^{1}H-{}^{13}C$ NMR correlations have been employed to unambiguously assign ^{1}H and ^{13}C signals of the same organic groups.

Acknowledgment. The European Commission is acknowledged for support through the EEC ARI contract HPRI-CT-1999-00042. Italian MIUR (PRIN contract no. 2002035342 and FIRB contract no. RBNE01P4JF) and French CNRS are acknowledged for financial support. Franck Fayon (Orléans) is also acknowledged for his preliminary work on the BABA experiments.

Supporting Information Available: Comparison between the percentages corresponding to a random distribution of units with the experimental ones; asssignment of the chemical shifts observed in the hybrid samples by ^{13}C CP MAS experiments; comparison between 1D BABA spectra recorded for Ge0T3G7; 2D BABA spectra recorded for Ge0T3G7; 2D spectrum of Figure 8 showing the smallest correlations; and data from Integrated Spectral Data Base System for Organic Compounds (SBDS) (pdf). This material is available free of charge via the Internet at http://pubs.acs.org.

CM047765G